



# NONLINEAR RESPONSE SPECTRUM FOR SYSTEMS WITH LOCALIZED NONLINEARITIES

MICHEL KAHAN

Laboratoire des Matériaux et des Structures du Génie Civil (LCPC/CNRS)

2 allée Kepler, 77420 Champs sur Marne, FRANCE

**Abstract:** This paper presents a nonlinear response spectrum method for MDOF systems with localized nonlinearities. Representative of such systems are bridges with nonlinearities localized at the bearings and at the base of the piers. The method is based on the stochastic averaging linearization technique: response of the equivalent linear system is obtained from linear response spectrum analysis. Since equivalent properties of the nonlinear elements depend on characteristics of the response (amplitude, average frequency, etc.), an iterative scheme is needed. An efficient algorithm making use of the localization of the nonlinearities is presented. The technique relies entirely on a given linear response spectrum and on the constitutive relations of the nonlinear elements. An example highway bridge with nonlinearities localized at the base of the piers is investigated. Results compare favorably with Monte-Carlo simulation results obtained by time-domain integration of the nonlinear response.

**Keywords:** response spectrum, localized nonlinearities, equivalent linearization, stochastic averaging.

## GENERAL FRAMEWORK

It is assumed that the structure dealt with behaves essentially in a linear elastic fashion except at a finite and small number of locations. In earthquake engineering this is commonly achieved if the structure is built according to the capacity design method: a number of elements (plastic hinges or special dissipative devices) are chosen to behave nonlinearly while the rest of the structure is designed to behave in an essentially linear elastic fashion. The capacity design method is however based on an equivalent static analysis, given forces that are derived from an elastic dynamic analysis. The following nonlinear response spectrum method retains the assumption that the nonlinearities are localized within specific and known members which will be called connections or potential plastic hinges hereafter, and that the rest of the structure remains linear elastic. The analysis is however carried out in a dynamic framework. The nonlinear connections are replaced by equivalent linear elements in order to be able to use a linear response spectrum analysis. The following section describes the stochastic averaging technique which is an appropriate method to linearize hysteretic nonlinear elements provided the response is narrow banded. The equivalent properties depend of the yet unknown response statistics. To take advantage of the linear properties of the remaining parts of the structure, a single modal analysis is performed with relaxed boundary conditions at the location of the nonlinear elements. The use of a limited number of modes of this "unconnected" structure as representative of the dynamic behavior of the linear substructures makes the subsequent analysis particularly efficient: equivalent linear elements are added, coupling the substructures and therefore the previously computed modes. A new set of eigenmodes is computed and a response spectrum analysis is performed. From the response of the equivalent linear elements, a new set of equivalent linear properties are calculated and the analysis is

## STOCHASTIC AVERAGING FOR A BILINEAR COMPONENT

First developed by Caughey (1960, 1963) the stochastic averaging method is based on temporal averages over hysteretic cycles whose characteristics vary slowly with time which is typical of narrow banded responses. For a complete description of the method, see Roberts and Spanos (1990), Igusa and Sinha (1989,1991). The nonlinear restoring force  $F(x, \dot{x})$  is replaced by an equivalent linear spring and dashpot parallel system  $F_{eq}(t) = c_{eq}\dot{x}(t) + k_{eq}x(t)$  where the equivalent coefficients are computed to minimize the error  $\varepsilon = F(t) - F_{eq}(t)$  during one cycle. To do so, a Van der Pol transformation is applied to the displacement variable  $x$  :

$$x(t) = A(t) \cos(\omega_{eq}t + \phi(t)) \quad , \quad \dot{x}(t) = -\omega_{eq}A(t) \sin(\omega_{eq}t + \phi(t)) \quad (1)$$

Assuming the response to be narrow banded, the amplitude  $A(t)$  and phase angle  $\phi(t)$  of the response vary slowly with time and may be taken as constants over one cycle. Solutions of the quadratic minimization problem :

$$\min_{\beta_{eq}, \omega_{eq}} \left\{ E \left[ \oint_{1cycle} \varepsilon^2 \right] \right\} \quad (2)$$

the parameters of the equivalent linear component are (Igusa and Sinha 1991) :  $k_{eq} = 2 \frac{E[C(A)]}{E[A^2]}$  and  $c_{eq} = c + 2 \frac{E[S(A)]}{\omega_{eq}E[A^2]}$ , where  $c$  accounts for viscous damping in addition to the hysteretic damping and

$$C(A) = \frac{A}{2\pi} \int_0^{2\pi} F[A \cos \theta] \cos \theta d\theta \quad , \quad S(A) = -\frac{A}{2\pi} \int_0^{2\pi} F[A \cos \theta] \sin \theta d\theta \quad (3)$$

The quantity  $S(A)$  has a physical interpretation :  $2\pi S(A)$  measures the dissipated energy per hysteretic loop. Note that  $\omega_{eq}$  is the average frequency of the narrow banded response. It may be defined according to Rice's formula as  $\omega_{eq} = \sqrt{\frac{\lambda_2}{\lambda_0}}$  where  $\lambda_m$  is the  $m^{th}$  spectral moment  $\lambda_m = \int_{-\infty}^{+\infty} \omega^m S_x(\omega) d\omega$ . The analytical expression of the hysteretic loop depends on the amplitude  $A$  of the oscillation only. Since the latter is an outcome of the response statistics, it is clear that an iterative procedure is needed. Note also that the response of the linear equivalent system to a Gaussian excitation is also Gaussian. In that case, it can be shown that for stationary processes, the amplitude follows a Rayleigh distribution  $f(A) = \frac{A}{\sigma^2} \exp(-\frac{A^2}{2\sigma^2})$ .

In the case of bilinear hysteretic restoring force shown on Figure 1, the equivalent spring and dashpot are obtained in closed form :

$$k_{eq} = k_o \left\{ \frac{1}{2} \int_0^{\frac{x_y}{\sigma_x}} a^3 e^{-\frac{a^2}{2}} da + \frac{1}{2} \int_{\frac{x_y}{\sigma_x}}^{+\infty} a^3 \left( \alpha + (1 - \alpha) \frac{\theta - \frac{1}{2} \sin(2\theta)}{\pi} \right) e^{-\frac{a^2}{2}} da \right\} \quad (4)$$

$$c_{eq} = c + \sqrt{\frac{2}{\pi}} \frac{(1 - \alpha) k_o x_y}{\omega_{eq} \sigma_x} \operatorname{erfc} \left( \frac{x_y}{\sqrt{2}\sigma_x} \right) \quad \text{where} \quad \operatorname{erfc}(X) = \frac{2}{\sqrt{\pi}} \int_X^{+\infty} \exp(-t^2) dt \quad (5)$$

where  $k_o$  is the initial elastic tangent stiffness,  $\alpha$  the post-yield to pre-yield stiffness ratio,  $x_y = F_y/k_o$  is the yield displacement (yield strength divided by the elastic tangent stiffness) and  $\theta = \cos^{-1}(1 - 2x_y/A)$ .

For engineering purposes, one needs the ductility demand in terms of maximum displacement. This is dealt with in the following sections. An equally interesting index in case of repeated hysteretic cycles is the equivalent energy dissipation ductility factor  $\mu_{energy}$ , equal to the displacement ductility of a monotonically loaded elasto-plastic component with the same yield strength and initial stiffness as the actual component and that dissipates the same amount of energy (Mahin and Bertero 1981). Namely,

$$\mu_{energy} = \frac{\text{Dissipated Energy}}{F_y x_y} + 1 = \frac{W_D}{k_o x_y^2} + 1 \quad (6)$$

Here, the expected dissipated energy per cycle  $E[W_D]$  is obtained in closed form and with the average number of cycles in the time interval  $[0, T]$ ,  $\frac{T\omega_{eq}}{2\pi}$ , the equivalent energy dissipation ductility factor becomes :

$$\mu_{energy} = 1 + \frac{T\omega_{eq}}{2\pi} \frac{E[W_D]}{k_o x_y^2} = 1 + T\omega_{eq} \sqrt{\frac{2}{\pi}} (1 - \alpha) \frac{\sigma_x}{x_y} \operatorname{erfc} \left( \frac{x_y}{\sqrt{2}\sigma_x} \right) \quad (7)$$

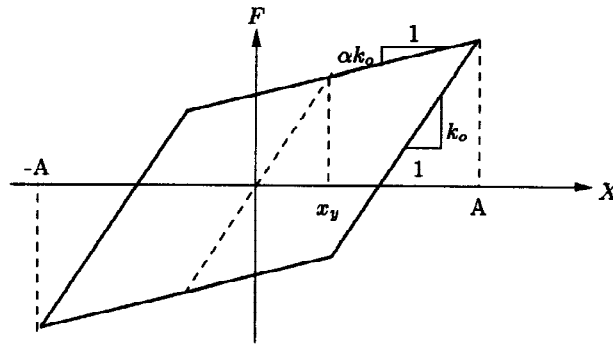


Figure 1: Bilinear hysteretic loop

## MODAL SYNTHESIS

As mentioned earlier, if the capacity design method is used, the structure remains mostly linear during strong shaking except at prescribed locations. The motion of each linear component may be described on the basis of its natural modes. Therefore the original structure is split into linear subsystems which in a first stage are assumed not to be connected. In other words, potential plastic hinges are replaced by true hinges, bearings (that partially isolate translational degrees of freedom) are replaced by perfectly sliding elements (with no friction). More generally nonlinear elements are replaced by relaxed boundary conditions between subsystems. The relaxation is only introduced in the direction of the original nonlinearity; thus, in the potential plastic hinge case, only the rotation is relaxed, not the translations. It is also assumed that the linear substructures are classically damped.

In a second stage, equivalent linear connections are introduced between subsystems, and the subsystem modes are used to build up the modes of the complete equivalent linear system. Eventually, a linear response spectrum is used to obtain structural responses. Recall that characteristics of connections depend on the amplitude of the response and therefore an iterative procedure is needed.

### Modal basis of the unconnected system

Let  $M$ ,  $C$  and  $K$  be the assembled mass, damping and stiffness matrices of the independent free subsystems. Namely,

$$M = \text{diag} \left\{ M_1 \quad M_2 \quad \cdots \quad M_n \right\} \quad C = \text{diag} \left\{ C_1 \quad C_2 \quad \cdots \quad C_n \right\} \quad K = \text{diag} \left\{ K_1 \quad K_2 \quad \cdots \quad K_n \right\} \quad (8)$$

where  $M_i$ ,  $C_i$  and  $K_i$  are mass, damping and stiffness matrices of subsystem  $i$ . Let  $\Phi$  be the modal matrix of the unconnected system  $\Phi = \text{diag} \left\{ \Phi_1 \quad \Phi_2 \quad \cdots \quad \Phi_n \right\}$ . It is assumed that the local modes are normalized so that  $\Phi^T M \Phi = \text{Id}$ ,  $\Phi^T K \Phi = \text{diag} \{ \omega_i^2 \}$  and since the local modes are classically damped  $\Phi^T C \Phi = \text{diag} \{ 2\zeta_i \omega_i \}$ . The second order differential equation of the unconnected system excited by a base ground motion  $\ddot{u}_g$

$$M\ddot{X} + C\dot{X} + KX = r\ddot{u}_g \quad (9)$$

can be turned into the augmented (in size) first order differential equation :

$$Y = \begin{Bmatrix} \dot{X} \\ X \end{Bmatrix} \quad A\dot{Y} + BY = R\ddot{u}_g \quad \text{where} \quad A = \begin{bmatrix} & M \\ M & C \end{bmatrix} \quad B = \begin{bmatrix} -M & \\ & K \end{bmatrix} \quad R = \begin{Bmatrix} 0 \\ r \end{Bmatrix} \quad (10)$$

Using the subsystem modes,  $X = \Phi V$ ,  $\dot{X} = \Phi \dot{V}$ , or  $\nu = \begin{Bmatrix} \dot{V} \\ V \end{Bmatrix}$   $Y = \begin{bmatrix} \Phi & 0 \\ 0 & \Phi \end{bmatrix} \nu$ , one finds :

$$A_0 \dot{\nu} + B_0 \nu = R_0 \ddot{u}_g \quad \text{where} \quad A_0 = \begin{bmatrix} 0 & \text{Id} \\ \text{Id} & \text{diag} \{ 2\zeta_i \omega_i \} \end{bmatrix}, \quad B_0 = \begin{bmatrix} -\text{Id} & \\ & \text{diag} \{ \omega_i^2 \} \end{bmatrix}, \quad R_0 = \begin{Bmatrix} 0 \\ \Phi^T r \end{Bmatrix}$$

Given that modes are mass-normalized, the lower part of  $R_0$  is the set of the modal participation factors. The reduced dynamic matrices  $A_0$  and  $B_0$  will be used to construct in a simple way the eigenmodes of the connected system.

### Additional spring or dashpot

An equivalent linear element (spring or dashpot) is added between two substructures and more specifically between the degrees of freedom  $i$  and  $j$  (in the original space). Let  $\mathbf{l}$  be the *link vector*, that is a vector of zeros except for rows  $i$  and  $j$  where it takes respectively the values 1 and  $-1$ . Let  $\alpha_s$  [resp.  $\alpha_d$ ] the value of the added spring [resp. dashpot] constant. The system matrices expressed in the original space and in the space of unconnected modes change in the following way : if a spring of constant  $\alpha_s$  is added,  $\mathbf{K}' = \mathbf{K} + \alpha_s \mathbf{l} \mathbf{l}^T$ ,  $\mathbf{B}' = \mathbf{B} + \begin{bmatrix} \mathbf{0} & \mathbf{0} \\ \mathbf{0} & \alpha_s \mathbf{l} \mathbf{l}^T \end{bmatrix}$ , and  $\mathbf{B}'_0 = \mathbf{B}_0 + \begin{bmatrix} \mathbf{0} & \mathbf{0} \\ \mathbf{0} & \alpha_s \mathbf{l}_0 \mathbf{l}_0^T \end{bmatrix}$  where  $\mathbf{l}_0 = \Phi^T \mathbf{l}$  is the link vector expressed in the basis of the unconnected modes; if a dashpot of constant  $\alpha_d$  is added,  $\mathbf{C}' = \mathbf{C} + \alpha_d \mathbf{l} \mathbf{l}^T$ ,  $\mathbf{A}' = \mathbf{A} + \begin{bmatrix} \mathbf{0} & \mathbf{0} \\ \mathbf{0} & \alpha_d \mathbf{l}_0 \mathbf{l}_0^T \end{bmatrix}$ , and  $\mathbf{A}'_0 = \mathbf{A}_0 + \begin{bmatrix} \mathbf{0} & \mathbf{0} \\ \mathbf{0} & \alpha_d \mathbf{l}_0 \mathbf{l}_0^T \end{bmatrix}$ . Once all connections have been incorporated, the state matrices are :

$$\mathbf{A}_0 = \begin{bmatrix} \mathbf{0} & \mathbf{Id} \\ \mathbf{Id} & \text{diag}\{2\zeta_i \omega_i\} + \sum_k \alpha_{d,k} \mathbf{l}_{0,k} \mathbf{l}_{0,k}^T \end{bmatrix} \quad \mathbf{B}_0 = \begin{bmatrix} -\mathbf{Id} & \mathbf{0} \\ \mathbf{0} & \text{diag}\{\omega_i^2\} + \sum_j \alpha_{s,j} \mathbf{l}_{0,j} \mathbf{l}_{0,j}^T \end{bmatrix} \quad (11)$$

### Modal basis of the connected system

To solve equation (10), one needs the eigenvectors of the system

$$\mu \mathbf{A} \psi + \mathbf{B} \psi = \mathbf{0} \quad \text{or} \quad \mu \mathbf{A}_0 \psi_0 + \mathbf{B}_0 \psi_0 = \mathbf{0} \quad \text{where} \quad \psi = \begin{bmatrix} \Phi & \mathbf{0} \\ \mathbf{0} & \Phi \end{bmatrix} \psi_0 \quad (12)$$

The small size eigenproblem  $(\mathbf{A}_0, \mathbf{B}_0)$  can be solved easily and because it is associated to nonclassical damping (recall that there are localized dashpots), it produces complex conjugate eigenvectors and eigenvalues.

### RESPONSE SPECTRUM

For a response quantity expressed as a linear combination of the displacement degrees of freedom of the structure  $\mathcal{E}(t) = \mathbf{q}^T \mathbf{X}(t) = \begin{bmatrix} \mathbf{0} & \mathbf{q}^T \end{bmatrix} \mathbf{Y}(t)$ , the modal participation factors are

$$b_i = \frac{\psi_i^T \mathbf{R}}{\psi_i^T \mathbf{A} \psi_i} \begin{bmatrix} \mathbf{0} & \mathbf{q}^T \end{bmatrix} \psi_i = \frac{\psi_{0,i}^T \mathbf{R}_0}{\psi_{0,i}^T \mathbf{A}_0 \psi_{0,i}} (\mathbf{q}^T \Phi) \psi_{0d,i} \quad (13)$$

Igusa, Der Kiureghian and Sackman (1983,1984) proposed a response spectrum method for non-classically damped systems based on the assumptions that the input is a wide band signal with a long stationary duration (i.e. several times longer than the fundamental period) and that the significant modes lie within the dominant frequency range of excitation. For a ground motion specified in terms of a linear displacement response spectrum  $D(\omega, \zeta)$ , the mean peak response is approximately:

$$E_\tau [|\mathcal{E}|] = \left[ \sum_{i=1}^q \sum_{j=1}^q [C_{ij} \rho_{0,ij} - D_{ij} \eta_{0,ij} w_{1,ij} + E_{ij} \rho_{2,ij} w_{2,ij}] D_\tau(\omega_i^*, \zeta_i^*) D_\tau(\omega_j^*, \zeta_j^*) \right]^{1/2} \quad (14)$$

where  $C_{ij} = a_i a_j$ ,  $D_{ij} = (a_i c_j - a_j c_i)$ ,  $E_{ij} = c_i c_j$ ,  $a_i = -2 \text{Re}(b_i \bar{\mu}_i)$ ,  $c_i = 2 \text{Re}(b_i)$  and

$$\rho_{0,ij} \approx R_{ij} [4\zeta_a + \zeta_d \omega_d / \omega_a] \quad \rho_{2,ij} \approx R_{ij} [4\zeta_a - \zeta_d \omega_d / \omega_a] \quad R_{ij} = \frac{\omega_a^2 \sqrt{\zeta_i \zeta_j}}{\omega_a^2 + 4\zeta_a^2 \omega_a^2} \quad (15)$$

with  $\omega_a = (\omega_i^* + \omega_j^*)/2$ ,  $\zeta_a = (\zeta_i^* + \zeta_j^*)/2$ ,  $\omega_d = \omega_i^* - \omega_j^*$ , and  $\zeta_d = \zeta_i^* - \zeta_j^*$

$$\eta_{m,ij} = 2R_{ij} \frac{\omega_d}{\omega_a} \quad , \quad w_{m,ij} = \begin{cases} (\omega_i^* \omega_j^*)^{m/2} & \text{m even} \\ (\omega_i^* \omega_j^*)^{m/2} \left[ \left(1 - \frac{2\zeta_i^*}{\pi}\right) \left(1 - \frac{2\zeta_j^*}{\pi}\right) \right]^{1/2} & \text{m odd} \end{cases} \quad (16)$$

With the maximum response and an expression for the peak factor (Der Kiureghian 1980), it is possible (Igusa and Der Kiureghian 1983) to derive the standard deviation  $\sigma_x$ , spectral moments  $\lambda_m$  and the average frequency  $\omega_{eq} = \sqrt{\lambda_2/\lambda_0}$  of the relative displacement of each equivalent linear element. These are used to update the equivalent linear properties of the nonlinear connections. The modal synthesis and the response spectrum analysis are performed again until convergence. It is important to realize that the iterative process is limited to a small scale system thanks to the use of a limited number of “unconnected” modes. It is therefore very efficient and fast.

## APPLICATIONS

### *Consistency with the inelastic response spectrum*

In this section the response spectrum based on the stochastic averaging method is compared with the inelastic response spectrum method widely used in earthquake engineering but which only applies to single degree of freedom elasto-plastic oscillators. The comparison is based on the behavior factor  $q$  obtained from both methods. For the response spectrum based on the stochastic averaging method, the behavior factor is computed in the following way. Given a frequency  $\omega_0$ , a damping ratio  $\zeta_0$ , and site conditions, the maximum relative displacement  $d_{max}^{lin}$  of the linear oscillator is computed from a response spectrum, as well as the standard deviation  $\sigma_x$  thanks to the peak factor. The equivalent linear properties of the elasto-plastic oscillator defined by a yield displacement  $x_y$  are (4, 5)  $\omega_{eq} = \omega_0 \sqrt{\frac{k_{eq}}{k_0}}$ ,  $\zeta_{eq} = \zeta_0 \frac{\omega_0}{\omega_{eq}} + \left(\frac{\omega_0}{\omega_{eq}}\right)^2 \frac{1}{\sqrt{2\pi}} \frac{x_y}{\sigma_x} \operatorname{erfc}\left(\frac{x_y}{\sqrt{2}\sigma_x}\right)$ . The yield displacement  $x_y$  is iteratively adjusted so that the ductility of the equivalent linear oscillator  $\mu = d_{max}^{eq}/x_y$  matches a target ductility  $\mu_{target}$ . The equivalent behavior factor is then

$$q = d_{max}^{lin}/d_{max}^{eq} (\omega_0/\omega_{eq})^2 \sqrt{(1 + 4\zeta_0^2)/(1 + 4\zeta_{eq}^2)}$$

The results are shown in Figure 2 for rock or firm soil conditions (French recommendations AFPS site S0). The behavior factor is presented versus the linear oscillator period for several target ductilities. In the low period range, the behavior factor goes to unity as expected. The right hand side figure shows that for short periods ( $T = 0.1s$ ) the behavior factor remains close to one (dashed line marked with +), independently the target ductility. In the long period range, the behavior factor slightly overestimates its theoretical limit, the target ductility. The right hand side figure shows that for long periods ( $T \geq 3s$ ), the behavior factor follows closely the target ductility (dashed line marked with  $\times$ ). In the intermediate range, it is expected that the behavior factor take the value  $q = \sqrt{2\mu - 1}$  (dashed line marked with circles). It can be seen that this relation is also approximately followed for intermediary periods ( $1s \leq T \leq 2s$ ). Thus, restricted to single degree of freedom oscillators, the response spectrum based on the stochastic averaging compares favorably with the widely used inelastic response spectrum. Of course, it covers many other applications, in particular more complex structures as will be seen in the next sections.

### *Highway bridge lateral excitation*

In this section and the following, the response of a highway bridge over the Gave de Pau, near Lourdes, in southern France is studied. Its total length is 248m, it has a composite deck, three concrete piers (2.5m x 2.5m) approximately 25m high. The deck is hinged on top of the piers, relative translations are blocked. At the abutment, lateral and vertical motions of the deck are blocked.

Thus the piers and the deck contribute to the lateral stiffness of the bridge. It is assumed, that for lateral ground excitation, plastic hinges may develop at the base of the piers only. Following the procedure presented herein, the model is hinged at the base of the piers and a modal analysis is performed. Note that because of the deck contribution to lateral stiffness, the hinges do not produce a rigid body mechanism. Also, there is only one substructure in this case. The main lateral modes are shown on Figure 3. Equivalent rotational springs and dashpots are then added at the base of the piers.

The maximum ductility demand in terms of plastic hinge rotations and energy dissipation through hysteretic cycles are presented in Table 1. Results are obtained from the response spectrum presented

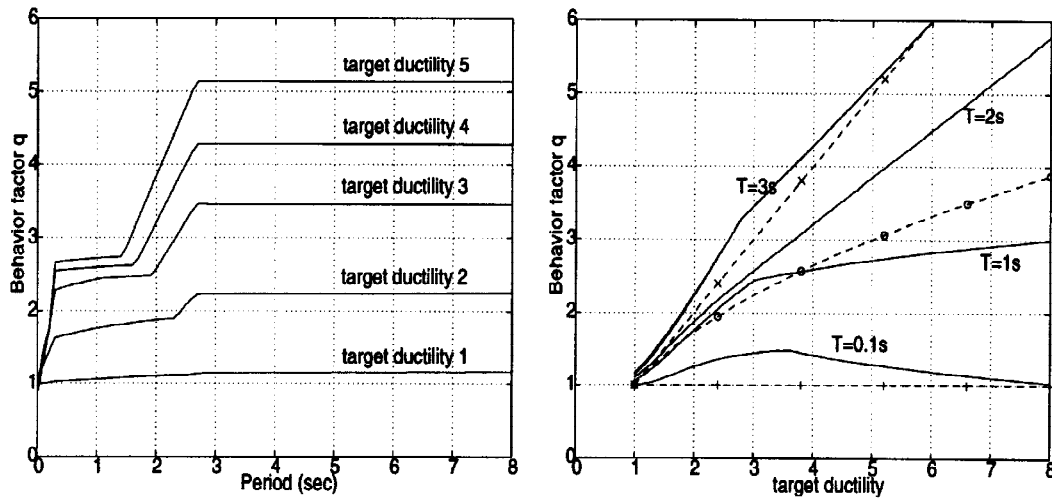


Figure 2: Behavior factor as found by the stochastic averaging based response spectrum

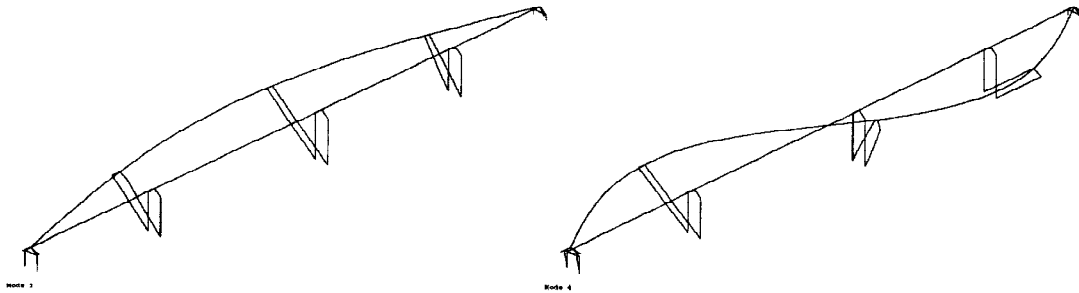


Figure 3: First two important lateral modes of the bridge hinged at the base of the piers

in this paper as well as from simulations. The latter were carried out by time-domain integration of the response of the same structure represented by the aforementioned modes and nonlinear relations reproducing the behavior of the elasto-plastic hinges. The ground accelerations were generated artificially in order to match (in the mean) the prescribed linear response spectrum (in this case, for soft soil, AFPS spectrum S3). Two levels of peak ground accelerations were used ( $a_g = 0.25g$  and  $a_g = 0.5g$ ).

For a peak ground acceleration of  $0.25g$ , the side piers (P1 and P3) remain essentially elastic and only the base of the central pier (P2) goes plastic with a mean maximum ductility demand of 1.45 and comparatively large energy dissipation through hysteretic cycles. The response spectrum technique reproduces these results with very good accuracy.

For a peak ground acceleration of  $0.5g$ , the base of the three piers go plastic and even with 400 simulations, the dispersion of the Monte-Carlo results remains high (20 to 30%). Again, the response spectrum technique gives very close results, in a much shorter time (a minute versus an overnight calculation).

### **Highway bridge longitudinal excitation**

For longitudinal motions, a simpler model of the bridge is adopted : the deck is assumed to be a rigid body moving longitudinally only. The piers are hinged to the deck. Again, plastic hinges are assumed to develop at the base of the piers. This time, if all pier bases are hinged, a mechanism develops. To avoid numerical problems in the initial modal analysis, small beam elements (or rotational springs) with very low bending stiffnesses (2% of the original elastic bending stiffness of the pier) are placed instead of the perfect hinges. The first mode thus obtained has a very low frequency and a shape very similar to that of the rigid body mode. Figure 4 shows this first mode along with three other modes, which are essentially local pier modes. The remaining analysis follows the procedure described in this paper.

Table 2 shows the results obtained for the rotation ductility and energy dissipation through hysteresis cycles at the base of the three piers. The ductility and energy dissipation are this time distributed over

$a_g = 0.25g$		P1	P2	P3
$\mu_d$	160 simulations	0.82 (8%)	1.45 (10%)	0.80 (8%)
	response spectrum	0.91 (15%)	1.56 (17%)	0.91 (16%)
$\mu_{energy}$	160 simulations	1.05 (5%)	6.20 (22%)	1.05 (5%)
	response spectrum	1.06	6.38	1.08
$a_g = 0.50g$		P1	P2	P3
$\mu_d$	400 simulations	1.21 (29%)	2.21 (22%)	1.19 (24%)
	response spectrum	1.33 (15%)	2.43 (16%)	1.41 (15%)
$\mu_{energy}$	400 simulations	1.93 (27%)	24.71 (17%)	1.97 (27%)
	response spectrum	2.47	24.11	3.27

Table 1: Lateral excitation, elasto-plastic hinges (coefficients of variation are within parentheses)

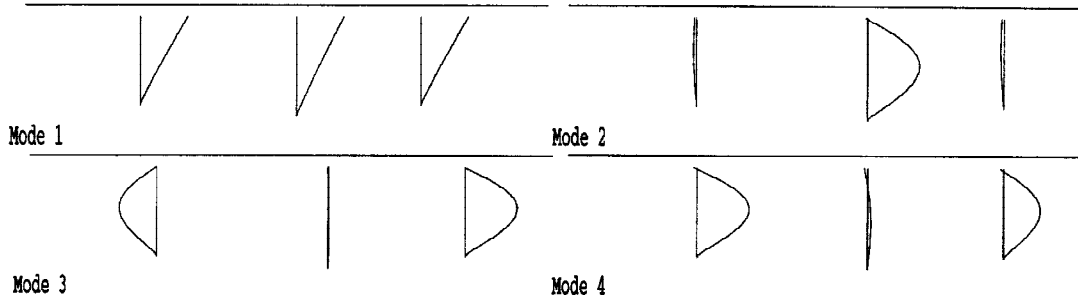


Figure 4: First four longitudinal modes of the bridge hinged at the base of the piers

all three piers, with a slight emphasis on the two side piers (P1 and P3) which are slightly shorter and yield earlier. For a peak ground acceleration of  $0.25g$ , Monte-Carlo simulations and the response spectrum technique give very comparable results in terms of displacement ductility. For a peak ground acceleration of  $0.50g$  the comparison is not as good but is still quite favorable. However, note the spread of the 280 simulations results : the coefficient of variation is higher than 50% for all piers, and it is therefore meaningless to expect a greater accuracy from any method. Note that the response spectrum technique locates very well the members that actually dissipate energy through hysteretic cycles, and gives quite accurate quantitative results.

$a_g = 0.25g$		P1	P2	P3
$\mu_d$	277 simulations	1.22 (20%)	0.94 (15%)	1.37 (19%)
	response spectrum	1.36 (19%)	1.10 (20%)	1.51 (19%)
$\mu_{energy}$	277 simulations	1.93 (41%)	1.10 (12%)	3.15 (46%)
	response spectrum	3.28	1.67	4.81
$a_g = 0.50g$		P1	P2	P3
$\mu_d$	280 simulations	2.44 (54%)	1.82 (54%)	2.54 (50%)
	response spectrum	2.09 (20%)	1.64 (17%)	2.24 (17%)
$\mu_{energy}$	280 simulations	10.47 (23%)	4.07 (26%)	14.31 (23%)
	response spectrum	12.65	5.66	15.59

Table 2: Longitudinal excitation, elasto-plastic hinges (coefficients of variation are within parentheses)

## CONCLUSION

The proposed linearization technique offers a compromise between the oversimplified inelastic response spectrum and the time consuming Monte-Carlo simulations, for MDOF structures with localized nonlinearities such as those designed according to the capacity design method. It is fast and simple since it requires a single modal analysis of the complete structure with relaxed boundary conditions, relies entirely on a given linear response spectrum and constitutive relations of the nonlinear elements. Elastoplastic relations were used as an example, but more sophisticated types of hystereses apply (Kahan 1996) as those based on the Bouc-Wen model (with a slightly different linearization technique though).

The proposed analysis has the following attributes: (a) it incorporates the uncertainties in the ground motion without using costly time-history analysis or Monte-Carlo simulations; (b) it allows the design engineer to perform parametric studies on the nonlinear elements at a reduced cost; (c) it provides insight and better understanding of the nonlinear behavior of the system and the relative influence of local nonlinearities on the global response of the structure.

## References

- Caughey, T. K. (1960). Random excitation of a system with bilinear hysteresis, *Journal of Applied Mechanics, ASME* **27**: 649–652.
- Caughey, T. K. (1963). Equivalent linearization techniques, *Journal of the Acoustical Society of America* **35**: 1706–1711.
- Der Kiureghian, A. (1980). Structural response to stationary excitation, *Journal of the Engineering Mechanics Division, ASCE* **106**: 1195–1213.
- Igusa, T. and Der Kiureghian, A. (1983). Response spectrum method for systems with non-classical damping, *4th Engineering Mechanics Division Specialty Conference*, West Lafayette, Indiana.
- Igusa, T. and Sinha, R. (1989). Probabilistic-based design of vibration absorbers in secondary systems, in H. Chung (ed.), *Current Topics in Structural Mechanics*, Vol. 179, ASME, PVP, pp. 27–34.
- Igusa, T. and Sinha, R. (1991). Response analysis of secondary systems with nonlinear supports, *Journal of Pressure Vessel Technology, ASME* **113**: 524–531.
- Igusa, T., Der Kiureghian, A. and Sackman, J. (1984). Modal decomposition method for stationary response of non-classically damped systems, *Earthquake Engineering and Structural Dynamics* **12**: 121–136.
- Kahan, M. (1996). Nonlinear response spectrum for systems with localized nonlinearities, *Technical Report RI96*, Laboratoire des matériaux et des structures du Génie Civil (LCPC/CNRS), Champs sur Marne, France.
- Mahin, S. and Bertero, V. (1981). An evaluation of inelastic seismic design spectra, *Journal of the Structural Division, ASCE* **107**(ST9): 1777–1795.
- Roberts, J. and Spanos, P. (1990). *Random vibration and statistical linearization*, John Wiley & Sons, England.